Received: 14 July 2022 | Revised: 19 August 2022 | Accepted: 30 September 2022

DOI: 10.1002/cac2.12369

CANCER COMMUNICATIONS Open Access

LETTER TO THE EDITOR

Malignant transformation by oncogenic K-ras requires IDH2-mediated reductive carboxylation to promote glutamine utilization

Dear Editor,

Oncogenic K-ras mutation plays a major role in malignant transformation and induces significant alterations in cancer cell metabolism [1–4]. However, the major molecular players mediating metabolic alterations during K-ras-driven cancer development remain elusive. The observations that tumorigenesis often requires multiple hits suggest that K-ras mutation likely needs the coordination of other molecular events that enable adaptive cellular metabolism for a full malignant transformation. Based on our previous study on the impact of K-ras on mitochondrial metabolism [1, 5] and our recent findings that mitochondrial isocitrate dehydrogenase 2 (IDH2) could promote the "reverse" flow of the tricarboxylic acid (TCA) cycle from α-KG to isocitrate and enhance the survival and proliferation of acute myeloid leukemia cells [6], we investigated the potential role of IDH2 in metabolic adaptation during K-ras-driven tumorigenesis.

We first used a tetracycline-inducible K-ras^{G12V} expression cell system (HEK293 T-Rex/K-ras cells) [1] to test the short-term and long-term K-ras induction effects on cell proliferation, tumor formation, and the associated changes in cellular metabolism. Acute induction of K-ras^{G12V} expression (K-ras/On) for relatively short periods (3 days to 2 weeks) resulted in a decrease in cell proliferation, whereas long-term induction of K-ras^{G12V} expression (K-ras/On for 6 weeks) led to an increase in cell growth (Figure 1A). Cells with acute K-ras^{G12V} induction were morphologically rounded and partially detached, exhibiting signs of stress. β-galactosidase (β-gal) staining revealed that a substantial portion of the cells was strongly positive for β-gal on day 3 to week 2 (3D-2W) (Figure 1B), suggesting that many of the stressed cells became senescent (3D-2W). With a prolonged K-ras^{G12V} induction, the cells seemed able to adapt to the oncogenic stress and showed healthy morphology without obvious senescence on week 6 (Figure 1B, panel 6W). Consistently, cells with acute K-ras^{G12V} activation could not form a significant number of colonies in soft agar, whereas cells with long-term induction of K-ras^{G12V} for 6 weeks could form colonies (Figure 1C). Analysis of IDH2 expression revealed a positive correlation between cell proliferation status and the temporal expression patterns of IDH2. Cells with short-term induction of K-ras^{G12V} resulted in a decrease in proliferation rate and a down-regulation of IDH2, whereas cells with long-term induction of K-ras^{G12V} exhibited a high proliferation rate and an up-regulation of IDH2 expression (Figure 1A-D and Supplementary Figure S1A). Such IDH2 expression pattern was consistently observed in another K-ras inducible cell system, where the hTERT-immortalized human pancreatic normal epithelial (HPNE) cells harboring inducible K-ras^{G12D} were tested for the expression of IDH2 and other relevant molecules (ACO2, GLS1, GLUD1) on day 3, week 2, and week 4 (Supplementary Figure S1B-C). In line with this unique IDH2 expression pattern, enzyme activity assays showed low IDH2 activity in cells with short-term (3D and 2W) K-ras activation and high IDH2 activity in cells with long-term (6W) K-ras induction, whereas no significant changes in IDH1 and IDH3 enzymes were observed in the same cells (Figure 1E). To explore the reason for IDH2 down-regulation during acute K-ras activation, we performed an IDH2 promoter activity assay in HEK293 cells with short-term K-ras induction (12 h, 24 h and 48 h). The cells transfected with a

Abbreviations: MTT, 3-(4,5-Dimethylthiazol-2-yl)-2,5-diphenyltetrazolium; TCA, tricarboxylic acid; OCR, oxygen consumption rate; IDH1-3, isocitrate dehydrogenase 1-3; α-KG, α-ketoglutarate; ACO2, mitochondrial aconitase; IHC, immunohistochemical; GSH, glutathione; GDH, glutamate dehydrogenase; Gln, glutamine; Glu, glutamate; GLUD1, glutamate dehydrogenase 1; GLS, glutaminase; OAA, oxaloacetate; Ac-coA, acetyl coenzyme A; Pyr, pyruvate; Fum, fumarate; Succ, succinate; HPNE, hTERT-immortalized human pancreatic normal epithelial; siRNA, small interfering RNA; shRNA, short-hairpin RNA; L, tumor length; W, tumor width; 3D, 3 days; 2W, 2 weeks; 6W, 6 weeks; qRT-PCR, real-time quantitative reverse transcription polymerase chain reaction; s.e.m., standard error of the mean.

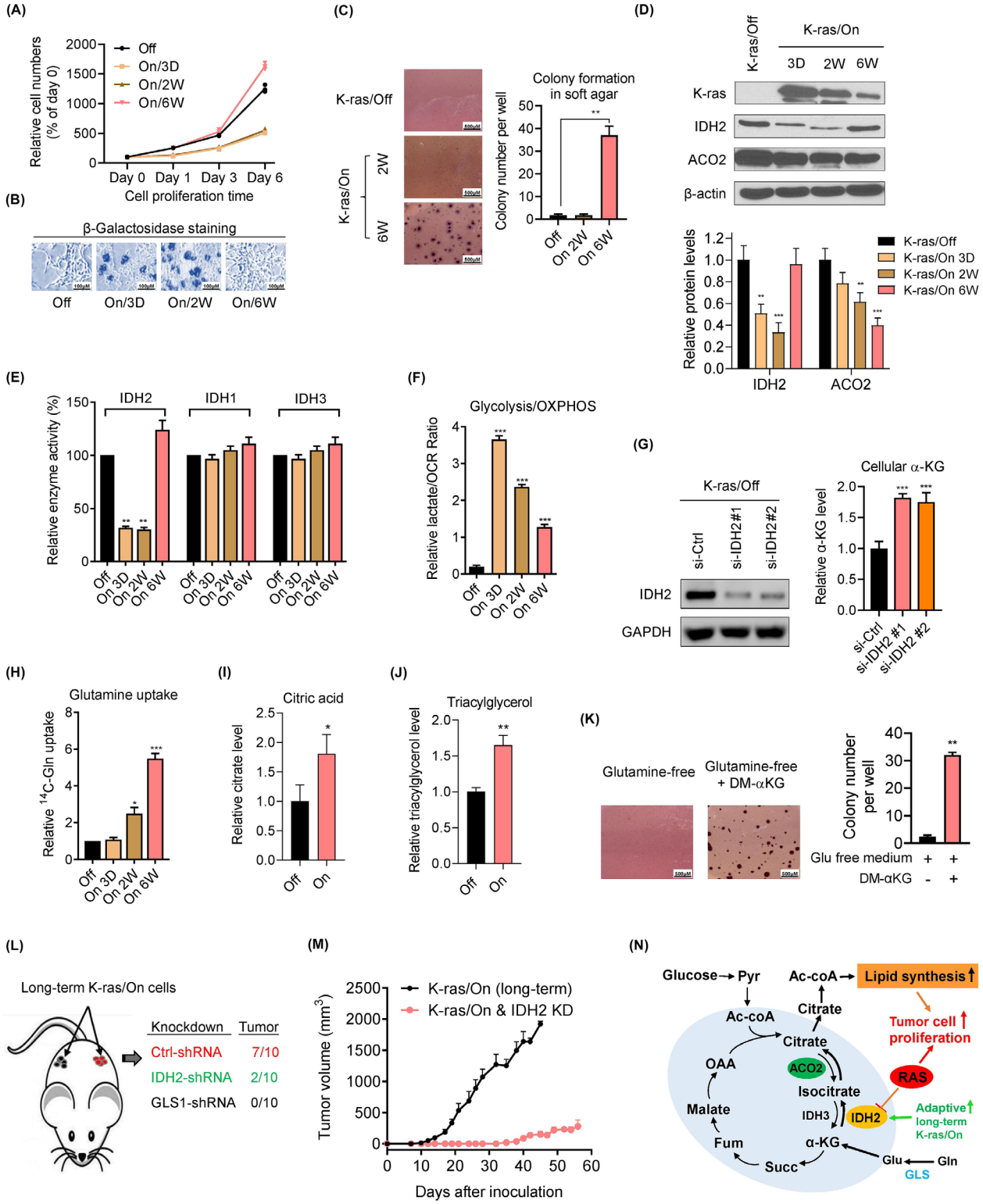

FIGURE 1 Malignant transformation induced by oncogenic K-ras requires IDH2-mediated reductive carboxylation to facilitate glutamine utilization for lipid synthesis. (A-B) The proliferation of HEK293 T-Rex/K-ras cells with or without induction of K-ras by doxycycline (20 ng/mL) for a short-term (3 days - 2 weeks) or long-term (6 weeks) as indicated. (A) Cell growth curves measured by MTT assays; (B) β-galactosidase staining assay showing cell senescence, scale bar: 100 μm; (C) Colony formation assay in the cells without or with induction of K-ras for the indicated times, scale bar: 500 μm. Left panel: representative images of colony formation assay; right panel: quantitation of colony formation assay; (D) Western blot analysis of IDH2 and ACO2 protein expression in HEK293 cells without or with K-ras induction as indicated (upper panel); quantification of protein levels analyzed by image J (low panel); (E) IDH enzyme activity assay in HEK293 cells with K-ras induction as indicated; (F) Ratio of lactate production/OCR in HEK293 cells with K-ras induction as indicated; (G)

luciferase reporter vector containing the IDH2 promoter exhibited a dramatic decrease (76%, 12 h; 90%, 24 h; 91%, 48 h) in luciferase activity when K-ras expression was induced (Supplementary Figure S1D), suggesting that K-ras could directly or indirectly suppress IDH2 expression at the transcriptional level. We also used real-time quantitative reverse transcription polymerase chain reaction (qRT-PCR) to measure the expression of endogenous IDH2 mRNA in cells with or without K-ras induction and found that the acute activation of K-ras (12-48 h) caused a 60%-80% decrease in IDH2 expression (Supplementary Figure S1E). Interestingly, using tumor tissues from a pancreatic cancer mouse model driven by *K-ras*^{G12D}*: Pdx-1-Cre* [7], we observed IDH2 upregulation in the tumor tissues at various stages of cancer development, with higher expression of IDH2 at the later stage of tumor development (Supplementary Figure S1F).

To examine the effect of K-ras activation with altered IDH2 expression on cellular metabolism, we measured oxygen consumption rate (OCR) and lactate production as the biochemical indicators of mitochondrial oxidative phosphorylation and cytosolic glycolysis, respectively. We found that the ratio of lactate production/OCR dramatically increased in cells with acute induction of K-ras^{G12V} (Figure 1F), reflecting a major decrease in mitochondrial oxidative phosphorylation likely due to IDH2 suppression that negatively impacted the TCA cycle. The highly elevated lactate/OCR ratio was eventually reduced after 6W induction of K-ras (Figure 1F), reflecting a recovery of mitochondrial oxidative metabolism with the re-expression of IDH2 during the metabolic adaptation. We then investigated the effects of IDH2 down-regulation on the TCA cycle. Strikingly, IDH2 knockdown by small interfering RNA (siRNA) in HEK293 cells caused a significant increase of α-KG (Figure 1G), suggesting that IDH2 might play a major role in the "reverse" (reductive) TCA cycle to produce citrate/isocitrate from α-KG, which was accumulated when IDH2 was knocked down. In line with this finding, IDH2 knockdown by siRNA resulted in the accumulation of α-KG in HPNE cells without K-ras induction or with long-term K-ras induction and a decrease in citrate and triacylglycerol levels (Supplementary Figure S1G-I). This observation led us to postulate that an increased expression of IDH2 in the long-term K-ras-activated cells might be required to promote glutamine utilization via conversion to α-KG and then to isocitrate/citrate through the reductive TCA metabolism for lipid synthesis to support cell proliferation. Indeed, glutamine uptake (Figure 1H) and generation of citrate (Figure 1I) and triacylglycerol (Figure 1J) were significantly increased in long-term K-ras/On cells (K-ras/On for 4 weeks, Supplementary Figure S1J). We noticed that the level of IDH2 expression (Figure 1E) was not quantitatively proportional to glutamine uptake (Figure 1H). A possible explanation would be that glutamine was used not only in the reductive TCA cycle catalyzed by IDH2 but also in other metabolic pathways, such as active glutathione (GSH) synthesis, to counteract the ROS stress induced by K-Ras activation. The elevated glutamine uptake at the early time points without elevated IDH2 likely reflects the active GSH synthesis unrelated to IDH2 expression. The dependency of K-ras/On cells on glutamine was evident since the cells could not form colonies in a glutamine-free medium (Figure 1K). The addition of cell-permeable

Effects of IDH2 knockdown by siRNA on the α-KG level in HEK293 cells. Left panel: western blot analysis of IDH2 protein expression; right panel: α-KG level in HEK293 cells harboring si-Ctrl or si-IDH2. α-KG was measured using an alpha-ketoglutarate assay kit (ab83431); (H) Glutamine uptake in HEK293 cells with K-ras induction at different time points, as indicated. The cells were cultured for 30 min with a medium supplemented with [U-^{14}C5] glutamine. Glutamine uptake was quantified by scintillation counting of the washed cells; (I) Citric acid analysis by LC-MS in HPNE cells with or without long-term (4 weeks) K-ras activation; (J) Triacylglycerol analysis by LC-MS in cells with or without long-term (4 weeks) K-ras activation; (K) Effect of DM-αKG on cell colony formation of HEK293 cells in a glutamine-free medium, scale bar: 500 μm; (L-M) Effects of IDH2 or GLS1 knockdown on tumor formation of long-term K-ras/On cells harboring control shRNA, shIDH2, or shGLS1 as indicated. The in vivo study design, tumor incidence, and tumor growth curves are shown; (N) Schematic illustration of the important role of IDH2-mediated reductive carboxylation to facilitate glutamine utilization for lipid synthesis during malignant transformation driven by oncogenic K-ras. Acute activation of K-ras suppresses IDH2 expression and causes stress. With long-term induction of K-ras, the cells eventually adapt and exhibit upregulation of IDH2, which promotes the reductive TCA cycle to facilitate utilization of glutamine through α-KG to citrate for lipid synthesis, leading to an increase in cancer cell proliferation. All images shown are representative, and data are shown as mean ± standard error of the mean (s.e.m.) of $n \geq 3$ independent experimental groups. Color code: Red, the effect of K-ras activation; green, adaptive responses; yellow, the role of IDH2 in response to K-ras activation. *$P < 0.05$; **$P < 0.01$; ***$P < 0.001$ (two-tailed Student's *t*-test). Abbreviations: MTT: 3-(4,5-Dimethylthiazol-2-yl)-2,5-diphenyltetrazolium; TCA: tricarboxylic acid; OCR: oxygen consumption rate; siRNA: small interfering RNA; shRNA: short-hairpin RNA; IDH1-3: isocitrate dehydrogenase 1-3; α-KG: α-ketoglutarate; ACO2: mitochondrial aconitase; IHC: immunohistochemical; GSH: glutathione; GDH: glutamate dehydrogenase; Gln: glutamine; Glu: glutamate; GLUD1: glutamate dehydrogenase 1; GLS: glutaminase; OAA: oxaloacetate; Ac-coA: acetyl coenzyme A; Pyr: pyruvate; Fum: fumarate; Succ: succinate; HPNE: hTERT-immortalized human pancreatic normal epithelial; 3D: 3 days; 2W: 2 weeks; 6W: 6 weeks; qRT-PCR: real-time quantitative reverse transcription polymerase chain reaction; s.e.m.: standard error of the mean.

DM-αKG to the glutamine-deprived cells significantly promoted colony formation (Figure 1K), further confirming the importance of this metabolic pathway to support cell proliferation in long-term K-ras/On cells. Consistent with the active utilization of glutamine, the expression levels of glutaminase 1 (GLS1, which converts glutamine to glutamate) and glutamate dehydrogenase 1 (GLUD1, which converts glutamate to α-KG) were significantly elevated in long-term K-ras-activated cells (Supplementary Figure S1K).

The role of IDH2 and GLS1 in supporting K-ras-driven tumor growth in vivo was then tested in animal experiments. Athymic nude mice were inoculated subcutaneously on the flanks with long-term (2 months) K-ras/On cells stably transfected with shIDH2, shGLS1, or control short-hairpin RNA (shRNA) vectors. The rates of tumor formation and tumor growth were measured as illustrated in Figure 1L. Seven out of ten mice inoculated with the long-term K-ras/On cells harboring control shRNA formed tumors and exhibited rapid growth. In contrast, only 2 of 10 mice inoculated with long-term K-ras/On cells harboring IDH2-shRNA formed tumors with a slow growth rate (Figure 1M). None of the animals inoculated with long-term K-ras/On cells harboring shGLS1 developed tumors (Figure 1L). Immunohistochemistry (IHC) analysis of the tumor tissues indicated that the tumors with long-term K-ras/On contained many more Ki-67 positive/proliferative cells than those harboring shIDH2 (Supplementary Figure S1L). Importantly, in vivo administration of GLS1 inhibitor, compound 968 (C968), significantly suppressed tumor growth in mice inoculated with long-term (6 weeks) K-ras/On cells (Supplementary Figure S1M). Altogether, these data suggest that cells with long-term K-ras activation were highly dependent on glutamine promoted by IDH2 and GLS1.

In conclusion, our study revealed an important role of mitochondrial IDH2 in K-ras-driven cancer development by promoting glutamine utilization through the reductive TCA cycle to generate isocitrate/citrate for lipid synthesis to support cell proliferation (Figure 1N). This conclusion is supported by a series of in vitro and in vivo evidence. As such, a metabolic intervention targeting IDH2 or/and GLS1 using the proper inhibitors might be a novel therapeutic strategy for the effective treatment of K-ras-driven cancers.

DECLARATIONS

ACKNOWLEDGMENTS

We thank the grant support from the National Key R&D Program of China (2020YFA0803300).

ETHICS APPROVAL AND CONSENT TO PARTICIPATE

This study does not involve any human participants, human data or human tissue; in vivo experiments using mice were reviewed and approved by the Institutional Animal Care and Use Committee (IACUC, the animal protocol#: ACUF#11-98-08136) of the University of Texas MD Anderson Cancer Center. The authenticity of this article has been validated by uploading the key raw data onto the Research Data Deposit public platform (www.researchdata.org.cn), with the approval RDD number as RDDB2022285199.

CONSENT FOR PUBLICATION

Not applicable.

DATA AVAILABILITY STATEMENT

The datasets used and/or analyzed during the current study are available from the corresponding authors upon reasonable request.

COMPETING INTERESTS

The authors declare that they have no competing interests.

FUNDING

This work was supported in part by a research grant from the National Key R&D Program of China (2020YFA0803300).

AUTHOR CONTRIBUTIONS

Rui Liu, Panpan Liu, Huichang Bi, Peng Huang and Jinyun Liu designed the study. Rui Liu, Jianhua Ling, Huiqin Zhang, Mingquan Zhang and Jinyun Liu conducted the experiments, collected and analyzed the data. Yumin Hu and Paul J Chiao analyzed the in vivo data. Rui Liu, Jinyun Liu and Peng Huang wrote the manuscript and revised the final manuscript. All authors read and approved the final manuscript.

Rui Liu[1,2]
Panpan Liu[1]
Huichang Bi[3]
Jianhua Ling[4]
Huiqin Zhang[1]
Mingquan Zhang[1]
Yumin Hu[1]
Paul J Chiao[4]
Peng Huang[1,5]
Jinyun Liu[1,5]

[1]*Sun Yat-sen University Cancer Center, State Key Laboratory of Oncology in South China, Collaborative*

Innovation Center for Cancer Medicine, Guangzhou, Guangdong 510060, P. R. China
[2]*School of Materials Science and Engineering, Sun Yat-sen University, Guangzhou, Guangdong 510275, P. R. China*
[3]*School of Pharmaceutical Sciences, Southern Medical University, Guangzhou, Guangdong 510515, P. R. China*
[4]*Department of Molecular and Cellular Oncology, The University of Texas MD Anderson Cancer Center, Houston, Texas 77030, USA*
[5]*Metabolic Research Platform, Center for Precision Medicine, Zhongshan School of Medicine, Sun Yat-sen University, Guangzhou, Guangdong 510080, P. R. China*

Correspondence
Jinyun Liu and Peng Huang, Sun Yat-sen University Cancer Center, State Key Laboratory of Oncology in South China, Collaborative Innovation Center for Cancer Medicine, Guangzhou 510060, Guangdong, P. R. China.
Email: liujinyun@sysucc.org.cn; huangpeng@sysucc.org.cn

Rui Liu and Panpan Liu authors contributed equally to this work

ORCID

Huichang Bi https://orcid.org/0000-0001-7094-2296
Mingquan Zhang https://orcid.org/0000-0002-1853-935X
Jinyun Liu https://orcid.org/0000-0002-4763-2684

REFERENCES

1. Hu Y, Lu W, Chen G, Wang P, Chen Z, Zhou Y, et al. K-ras(G12V) transformation leads to mitochondrial dysfunction and a metabolic switch from oxidative phosphorylation to glycolysis. Cell Res. 2012;22(2):399-412.
2. Son J, Lyssiotis CA, Ying H, Wang X, Hua S, Ligorio M, et al. Glutamine supports pancreatic cancer growth through a KRAS-regulated metabolic pathway. Nature. 2013;496(7443):101-5.
3. Wu TC, Liao CY, Lu WC, Chang CR, Tsai FY, Jiang SS, et al. Identification of distinct slow mode of reversible adaptation of pancreatic ductal adenocarcinoma to the prolonged acidic pH microenvironment. J Exp Clin Cancer Res. 2022;41(1):137.
4. Sela Y, Li J, Maheswaran S, Norgard RJ, Yuan S, Hubbi ME, et al. Bcl-xL enforces a slow-cycling state necessary for survival in the nutrient-deprived microenvironment of pancreatic cancer. Cancer Res. 2022;82(10):1890-908.
5. Meng N, Glorieux C, Zhang Y, Liang L, Zeng P, Lu W, et al. Oncogenic K-ras induces mitochondrial OPA3 expression to promote energy metabolism in pancreatic cancer cells. Cancers (Basel). 2019;12(1):65.
6. Zeng P, Lu W, Tian J, Qiao S, Li J, Glorieux C, et al. Reductive TCA cycle catalyzed by wild-type IDH2 promotes acute myeloid leukemia and is a metabolic vulnerability for potential targeted therapy. J Hematol Oncol. 2022;15(1):30.
7. Ling J, Kang Y, Zhao R, Xia Q, Lee DF, Chang Z, et al. KrasG12D-induced IKK2/beta/NF-kappaB activation by IL-1alpha and p62 feedforward loops is required for development of pancreatic ductal adenocarcinoma. Cancer Cell. 2012;21(1):105-20.

SUPPORTING INFORMATION

Additional supporting information can be found online in the Supporting Information section at the end of this article.